© 2020. Published by The Company of Biologists Ltd | Journal of Experimental Biology (2020) 223, jeb219832. doi:10.1242/jeb.219832

RESEARCH ARTICLE

Neural processing of linearly and circularly polarized light signal in a mantis shrimp *Haptosquilla pulchella*

Tsyr-Huei Chiou[1,*] and Ching-Wen Wang[1,2]

ABSTRACT

Stomatopods, or mantis shrimp, are the only animal group known to possess circular polarization vision along with linear polarization vision. By using the rhabdomere of a distally located photoreceptor as a wave retarder, the eyes of mantis shrimp are able to convert circularly polarized light into linearly polarized light. As a result, their circular polarization vision is based on the linearly polarized light-sensitive photoreceptors commonly found in many arthropods. To investigate how linearly and circularly polarized light signals might be processed, we presented a dynamic polarized light stimulus while recording from photoreceptors or lamina neurons in intact mantis shrimp *Haptosquilla pulchella*. The results indicate that all the circularly polarized light-sensitive photoreceptors also showed differential responses to the changing e-vector angle of linearly polarized light. When stimulated with linearly polarized light of varying e-vector angle, most photoreceptors produced a concordant sinusoidal response. In contrast, some lamina neurons doubled the response frequency in reacting to linearly polarized light. These responses resembled a rectified sum of two-channel linear polarization-sensitive photoreceptors, indicating that polarization visual signals are processed at or before the first optic lobe. Noticeably, within the lamina, there was one type of neuron that showed a steady depolarization response to all stimuli except right-handed circularly polarized light. Together, our findings suggest that, between the photoreceptors and lamina neurons, linearly and circularly polarized light may be processed in parallel and differently from one another.

KEY WORDS: Electrophysiology, Stomatopod, Polarization vision, Lamina, Visual neuropil

INTRODUCTION

Many animals, particularly invertebrates, possess photoreceptors that are sensitive to linearly polarized light (LPL; for review, see Cronin et al., 2014; Horváth, 2014). Their polarization sensitivity arises from intrinsically dichroic and well-aligned photopigments within each receptor (Moody and Parriss, 1961; Snyder, 1973). Among them, however, only a few animals such as mantis shrimp are known to have true polarization vision as a result of a visual system that can discern the composition of LPL (e.g. e-vector angle or degree of polarization) independent of color and brightness (Marshall and Cronin, 2014; Nilsson and Warrant, 1999; Schwind, 1984). As for color vision, theoretically, achieving true polarization vision requires the implementation of polarization-opponent neurons (Bernard and Wehner, 1977; Buchsbaum and Gottschalk, 1983; Cronin et al., 2014; Daw, 1973). In contrast, their unexpectedly low spectral resolution determined from behavioral experiments suggests that mantis shrimp might not have the color opponent system at all (Thoen et al., 2014). Consequently, we were interested to see how the polarized light information might be processed by the visual system of stomatopod crustaceans and thus support polarization vision.

In addition to linear polarization vision, it has been shown that some stomatopod crustaceans can discriminate the handedness of circularly polarized light (CPL) and thus possess circular polarization vision (Chiou et al., 2008; Gagnon et al., 2015; Templin et al., 2017). The compound eye of stomatopod crustaceans has three distinctive regions: a dorsal hemisphere, a ventral hemisphere and a mid-band. In stomatopods of the superfamily of Gonodactyloidea, Lysiosquilloidea, Pseudosquilloidea and Hemisquilloidea, the mid-band is composed of six rows of enlarged ommatidia (Manning et al., 1984; Porter et al., 2010). Receptors of the four dorsal-most mid-band rows (rows 1–4) are dedicated to color vision while receptors in rows 5 and 6 detect circularly polarized light (Chiou et al., 2008; Templin et al., 2017). Each ommatidium in mid-band rows 5 and 6 is composed of eight retinular cells in two-tiers (i.e. distal and proximal tier; Marshall et al., 1991a). The rhabdomere of the distal 8th retinular cell (R8) serves as an optical wave retarder which can convert CPL of opposite handedness into orthogonally oriented LPL. Afterwards, the LPL is detected by two groups of proximal retinular cells (i.e. R1, 4, 5 and R2, 3, 6, 7) depending on its e-vector angle (Chiou et al., 2008). However, the conversion of CPL to LPL relies on precise optics, which might be too large to fit into the eyes of relatively small species or sub-adults (Roberts et al., 2009; Templin et al., 2017). Consequently, the contrast between the signals in LPL-sensitive receptors is reduced, or could be maximized upon stimulation with elliptically polarized light (EPL) of a specific ellipticity. In other words, some of the stomatopods might have elliptical polarization vision that is tailored for a specific set of EPL at the photoreceptor level (Cronin et al., 2014). To date, stomatopod crustaceans are the only animal group known to possess elliptical polarization vision (Templin et al., 2017). Nevertheless, whether EPL-sensitive photoreceptors can form elliptical polarization vision that supports a behavioral function remains to be tested (Cronin et al., 2014).

While circular polarization vision was discovered more than a decade ago, aside from some behavioral studies and basic neuroanatomy, how CPL signals are processed in the eyes of mantis shrimp remains unknown (Thoen et al., 2017, 2018). One of the major challenges for tapping into neurons proximal to the photoreceptors is to produce the appropriate stimulus that can elicit their responses. By removing one of the polarizers from an LCD monitor, one can easily produce dynamic LPL patterns which can be perceived by mantis shrimp (Daly et al., 2016). In addition, the modified LCD monitor can produce a precise polarization pattern on demand and has been used for examining various aspects of polarization vision in animals such as

[1]Department of Life Sciences, National Cheng Kung University, Tainan 70101, Taiwan. [2]Queensland Brain Institute, University of Queensland, St Lucia, QLD 4072, Australia.

*Author for correspondence (thchiou@mail.ncku.edu.tw)

T.-H.C., 0000-0003-3504-5113

Received 6 December 2019; Accepted 16 October 2020

Journal of Experimental Biology (2020) 223, jeb219832. doi:10.1242/jeb.219832

crayfish, cuttlefish, mantis shrimp and human subjects (Cartron et al., 2013; Daly et al., 2016; Glantz and Schroeter, 2006; How et al., 2014; Pignatelli et al., 2011; Temple et al., 2012, 2015). Unfortunately, we failed to find a way to control CPL or EPL output of the LCD monitor, which made it inadequate as a source of stimulation. As the CPL-sensitive photoreceptors in mantis shrimp are confined in the mid-band, we hypothesized that a light stripe or even a point light source which produces a time-varying polarized light stimulus that mimics the mid-band scanning through its environment might be sufficient to specifically stimulate CPL processing neurons. In practice, both CPL and LPL can be seen as an extreme case of EPL. That is to say, any EPL can be decomposed into a specific mixture of CPL and LPL (Born and Wolf, 1999; Ivanoff and Waterman, 1958; Johnsen, 2012). As a result, it is possible to resolve EPL without ambiguity by incorporating both LPL and CPL detectors into one polarization visual system. Based on the same principle, it is theoretically possible to resolve the linear and circular component of the incoming light using a group of photoreceptors that are tuned to a specific set of EPLs.

Based on the spectral discrimination function acquired through behavior tests, it has been suggested that mid-band rows 1–4 of stomatopod crustaceans process color information without a color-opponent coding system (Thoen et al., 2014). Based on the shared lamina cartridges between mid-band rows 5 and 6 (Thoen et al., 2017), we hypothesized that the processing of CPL or EPL should be detectable at the level of the lamina. In blowflies, it has been suggested that the principal functions of lamina neurons are frequency filtering, amplification and antagonism (Laughlin and Osorio, 1989). For *Drosophila*, the center-surround opponent processing is known to occur at the synapses between photoreceptors and lamina monopolar neurons (Freifeld et al., 2013). However, we noted that both *Drosophila* and blowflies are dipterans with neural superposition eyes. The neural connection and the early visual signal processing are probably very different from those of mantis shrimp, which have true apposition eyes. Given that the mid-band rows 1–4 of mantis shrimp sense different spectral ranges from a narrow slice of the environment (Marshall et al., 1991b; Marshall and Land, 1993a), it is conceivable that center-surround opponency, if it exists at all, will be confounded by color signals. However, antagonism between outputs of rows 5 and 6 photoreceptors could be the first step for processing CPL or EPL. To find out where and how the polarized light signal might have been processed in the early stages, we used sharp microelectrode recordings from the retina and lamina of a mantis shrimp *Haptosquilla pulchella* (Miers 1880). Based on electrophysiological recordings, here we confirm that some of the photoreceptors in *H. pulchella* are sensitive to both LPL and CPL, which makes them EPL-sensitive receptors. In the lamina, we found neurons receiving inputs from two orthogonal polarization-sensitive channels. Additionally, while the photoreceptors are optimized for certain EPL, some neurons in the lamina are responsive only to the handedness of CPL. The results indicate that, owing to the EPL-sensitive photoreceptors, the circular and linear components of the polarized light might be processed separately at the lamina of stomatopods.

MATERIALS AND METHODS

Animals

Adult *Haptosquilla pulchella* (total length 2.3–3.5 cm) were collected by scuba diving between subtidal and 10 m depth from Kenting National Park, Pingtung County, Taiwan, under the permission granted by Kenting National Park, Construction and Planning Agency Ministry of the Interior, Taiwan. After being brought back to the laboratory, the mantis shrimp were identified, sexed, measured and kept in aquaria. Each aquarium was filled with artificial seawater and maintained at 25°C under natural light conditions. The animals were fed with prawn bits every other day. We used only freshly caught animals for electrophysiology recordings and care was taken to avoid newly molted individuals.

Histology

Stomatopods were anesthetized with ice-cold seawater, and their eyes were ablated and transferred to PEMS buffer (0.1 mol l^{-1} Pipes, 1 mmol l^{-1} EGTA, 0.5 mmol l^{-1} $MgCl_2$, 1.5% sucrose, pH 7.1). The cuticle and cornea of the eye stalk was removed while submersed in buffer. The remaining tissue was fixed with 4% glutaraldehyde in PEMS buffer at 4°C overnight, followed by dehydration in an ethanol series (30 min for each step), transferred to pure acetone, infiltrated with Durcupan ACM (44610, Sigma-Aldrich, St Louis, MO, USA) resin, and cured at 65°C for at least 48 h. Semi-thin sections of 1.5–2 µm thickness were cut with glass knives on a Reichert-Jung Ultracut E microtome and mounted on a glass slide with the help of ethylene glycol (Burnett, 1975). The sections were stained with 0.5% Toluidine Blue in 1% sodium borate solution, coverslipped and photographed under a compound microscope.

Electrophysiology recording

Intracellular recordings were performed inside a Faraday cage on a pneumatic vibration isolation table in a dark room. Fig. 1 shows the setup for *in vivo* intracellular recordings from *H. pulchella*. The recording chamber was made of a 250 ml round-bottom flask with one side removed to allow the insertion of the recording electrode (Fig. 1A). To prepare for recording, the animal was chilled in cold (~5°C) seawater. An opening was cut on the medial side of the eyestalk next to the mid-band cornea with a razor blade. The dorsal carapace of the animal was then glued to a spatula, which was retrofitted with a silicon rubber that sealed and held the animal in the recording chamber (Fig. 1B). After the recording chamber was filled with oxygenated artificial seawater the position of targeted eye was adjusted to the center of the flask while keeping the mid-band perpendicular to the air table.

Filamented glass tubing (GC120F-15, Warner Instruments, Holliston, MA, USA) and a micropipette puller (P-87, Sutter Instrument, Novato CA, USA) were used to fabricate the recording microelectrode. The resistances of electrodes ranged from 80 to 120 MΩ when filled with 1 mol l^{-1} KCl. To record from photoreceptors or lamina neurons, the electrode was adjusted such that the travel direction was roughly parallel to the basement membrane of mid-band ommatidia (Fig. 1C). The electrode was mounted on the headstage of an amplifier (Axoclamp 900A, Molecular Devices, San Jose, CA, USA) which was attached to a three-axis mechanical micromanipulator through a one-axis hydraulic micromanipulator (MHW-4, Narishige, Tokyo, Japan) for adjustment and advancement of the electrode into the tissue. The amplifier was set in current-clamp mode with bridge balance while the amplified signal was digitized by a multifunction I/O device (USB-6341, National Instruments, Austin, TX, USA). Both the amplifier and multifunction I/O device were connected to a PC with custom-written software for setting adjustment, stimulus control and data recording. Both the signal and the response were recorded at 10 kHz. The data were digitally filtered by applying a low-pass fifth-order Butterworth filter with a cut-off frequency of 350 Hz and a 60 Hz notch filter. The custom software is available upon request from the corresponding author.

Light stimulus

The light source of the stimulus was a 3 W high-power natural white (6500 K) light-emitting diode (LED, 2ES103CW14000001, Edixeon

Journal of Experimental Biology (2020) 223, jeb219832. doi:10.1242/jeb.219832

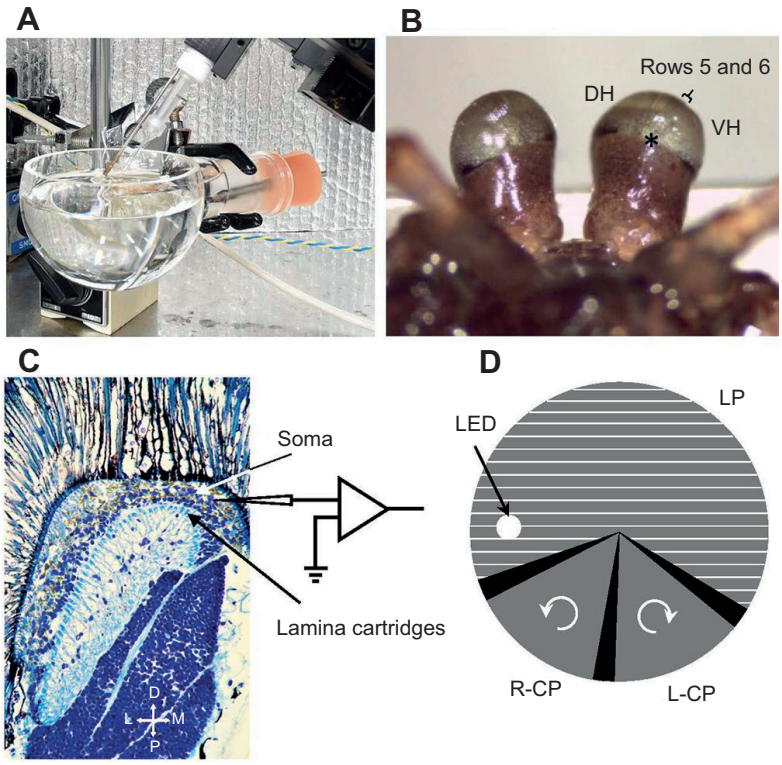

Fig. 1. Setup for recording polarized light responses of *Haptosquilla pulchella*. (A) Overview of the recording chamber and the recording electrodes. (B) View from the direction of the microelectrode showing the electrode insertion point (*). DH, dorsal hemisphere; VH, ventral hemisphere. Mid-band rows 5 and 6 are indicated. (C) Frontal section of the eye at mid-band level. The schematic diagram shows the approximate direction of electrode insertion. (D) Schematic diagram of the polarizer filter for producing the dynamic polarized light stimulus. View from the recording chamber; if the filter rotates counter-clockwise for 360 deg the animal will receive in tandem linearly polarized light (LPL) with the e-vector angle from 0 to 180 deg followed by left (L)-circularly polarized light (CPL), right (R)-CPL, and concluding with a brief moment of near-0 deg LPL.

Series, Edison Opto Corp., Taipei, Taiwan) driven at a constant current of 700 mA. The LED driver was controlled by the multifunction I/O device mentioned above which allowed programmable production of continuous illumination or light pulses. The light was polarized by passing through a modified linear polarizing filter (PL 52 mm, Tiffen Co., Hauppauge, NY, USA): two pieces of 1/4 λ retarder film (88-253, Edmund Optics, Barrington, NJ, USA) that each covered a 1/6 circular sector of the filter were glued onto the linear polarizing filter with mounting medium (Entellan, Merck, Darmstadt, Germany) to prevent the formation of interference fringes (Fig. 1D). Note that the retarder film is designed to have precisely 1/4 λ retardance at around 560 nm and retains adequate retardance between 450 and 650 nm. Stripes of opaque tape were then applied to mask the transition between retarders and the linear polarizer. By attaching the modified polarizing filter to a stepper motor (28BYJ-48, generic), it can produce LPL of all possible angles as well as CPL of both handedness in one rotation of the filter. While the rotation of the stepper motor is controlled by the computer, once started, its angular speed is fixed at approximately 3.6 rad s^{-1} in either direction.

After the electrode impaled a neuron or photoreceptor and a stabilized resting membrane potential was achieved, flashes of light at 1 Hz 50% duty cycle were delivered to check for signs of photoresponses. If the cell did respond to light, by either depolarization or hyperpolarization, its response to white light pulse was recorded as a baseline. Afterwards, the cell was subjected to a sequence of the polarized light stimuli. Viewing from the animal side, firstly, the polarizer rotated counter-clockwise which delivered LPL from near 0 to 180 deg followed by left-handed (L)-CPL and right-handed (R)-CPL, and ending with 0 deg LPL. After the membrane potential returned to the pre-stimulus level, the response of the same cell was recorded again but with the polarizer rotated clockwise to check for the consistency of the responses.

Timing of the stimuli

Two data traces were recorded simultaneously during the experiments: the amplified membrane potential and the voltage of the transistor–transistor logic (TTL) signal sent to the LED driver. The TTL signals were used to align traces between different recordings as the latencies of both the LED and the LED driver are negligible at the 10 kHz sampling rate. The synchronization between the illumination and the position of the rotating polarizer is achieved through counting steps of the stepper motor and the feedback of a photo interrupter, which detects the 'home flag' glued on the edge of the polarizer. To check for the consistency of timing and relative intensity of the stimulus, we used another LED (EDER-1LA3, Edixeon Series, Edison Opto Corp., Taipei, Taiwan) as a photodiode to acquire the calibration curves. The photodiode was waterproofed with hot-melt glue and submersed in pure water within the recording chamber in place of the animal's eyes. To simulate the recording conditions, the output of the photodiode was connected to the headstage of the amplifier through a resistor voltage divider. By adjusting the light source to various angles around the recording chamber, we acquired 336 timing calibration traces. The discrepancy between traces were determined by comparing the points immediately rising above or falling below half-maximum as a result of turning the LED on or off, or the obstruction of light by the opaque tape.

RESULTS

Properties of the stimuli

With the dynamic polarized stimulus, the recording chamber did not affect the intensity of the light. However, by moving the light source around the recording chamber, we found a phase shift of the stimuli for up to 26.4 ms. Based on the 3.6 rad s^{-1} rotation speed of the polarizer, the phase shift of the stimuli also represents a ±2.72 deg uncertainty in the e-vector angle of our LPL stimuli. Because of the bias in the timing of stimuli, we included two timing traces at the bottom of the results to facilitate data interpretation (Fig. 2, Int trace).

Responses of photoreceptors to polarized light

We successfully recorded dynamic polarized light responses from 40 photoreceptors of *H. pulchella*. As the LED does not produce

Journal of Experimental Biology (2020) 223, jeb219832. doi:10.1242/jeb.219832

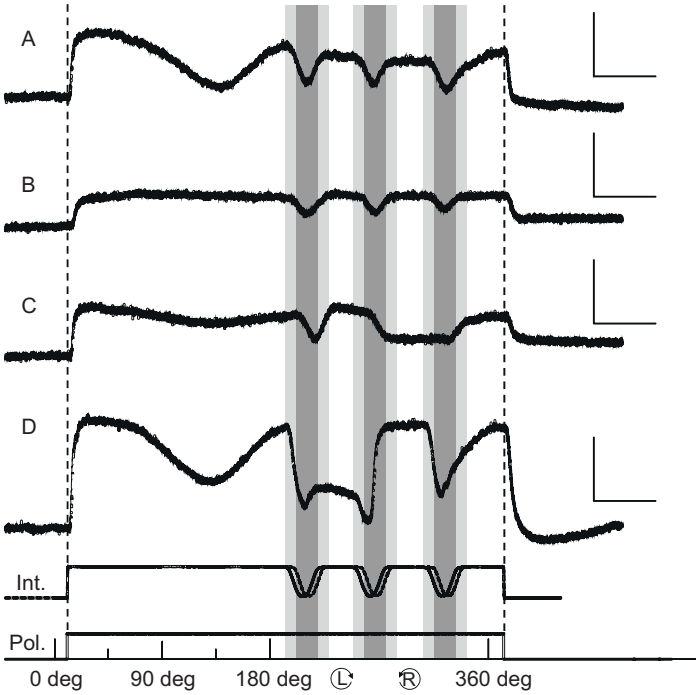

Fig. 2. Responses of *H. pulchella* photoreceptors to the time-varying polarized light stimulus. (A,B) Photoreceptors insensitive to CPL showed either the presence (A) or absence (B) of response fluctuation with the changing e-vector angle of LPL. (C,D) The membrane potential of CPL-sensitive photoreceptors showed a stronger depolarizing response to either L-CPL (C) or R-CPL (D) and minor fluctuations with the changing e-vector angle of LPL. For all the traces, the stimulus started with LPL with the e-vector angle changing from near 0 deg to slightly over 180 deg followed by L-CPL and R-CPL as indicated at the bottom (Pol.). Between different polarized stimuli, the LED was temporarily obscured by the opaque tape and the light intensity was reduced as shown in the intensity calibration trace (Int.) and indicated by the shaded area. The solid and dashed calibration traces represent the extreme cases of potential phase shift in the timing of the stimuli. The light-gray shading specifies potential bias of timing when the obstruction of the LED started or ended while the dark-gray shading indicates the overlapping of the light-gray regions. One revolution of the polarizer constituted a complete stimulus sequence, which takes approximately 1.75 s. Vertical scale bars: 10 mV; horizontal scale bars: 250 ms.

ultraviolet light, which is required to stimulate the R8 (Cronin et al., 1994), we assumed that all of the recorded photoreceptors were R1–7. Based on their responses to polarized light, these photoreceptors could be grouped into three types (Fig. 2). Twenty-three of the photoreceptors exhibited linear polarization sensitivity (type I photoreceptor; Fig. 2A), three showed equal responses to all the polarized light stimuli (i.e. polarized light insensitive; type II photoreceptor; Fig. 2B), and the other 14 photoreceptors exhibited circular polarization sensitivity with fluctuations to angle-varying LPL (type III photoreceptors; Fig. 2C,D). Among type III photoreceptors, six reacted to the L-CPL with a stronger depolarization response and were thus termed L-CPL receptors (Fig. 2C), while the other eight cells showed a significantly higher response to R-CPL, and were therefore called R-CPL receptors (Fig. 2D). According to the functional properties of the photoreceptors, it was assumed that type I, II and III responses were obtained from the photoreceptors of the hemispheres, mid-band rows 1–4 and mid-band rows 5–6, respectively.

Responses of lamina neurons to polarized light

Fig. 3 shows responses of various types of lamina neurons to flash and dynamic polarized light. We categorized the neurons based on their resemblance to the response profiles found in crayfish (Glantz and Bartels, 1994; Wang-Bennett and Glantz, 1987a,b). Of the 19 lamina neurons recorded, 14 were laminar monopolar cell-like neurons (LMCLNs; Fig. 3A–F), and the rest were lamina tangential-like neurons (Fig. 3G,H). Upon pulses of white light, all of the LMCLNs produced a graded hyperpolarization response consisting of an ‘on’ transient followed by a plateau (Fig. 3A,D). Whereas none of the recorded LMCLNs showed signs of circular polarization sensitivity, some of them did exhibit linear polarization sensitivity (Fig. 3E,F). Accordingly, the LMCLNs were further categorized based on the presence or absence of polarization sensitivity. Ten of the LMCLNs belonged to the first group, which did not show any differential responses to the changing e-vector (Fig. 3B,C), while the other four cells exhibited significant depolarization responses at two specific e-vector angles (Fig. 3E,F). That is to say, within a half-turn of the polarizer (0 to 180 deg), the polarized light-sensitive LMCLNs showed two depolarization episodes. For example, in Fig. 3E, two dips were found in the recorded waveform when the e-vector of the stimulus was approximately 45 and 135 deg. When the e-vector of the polarized light was presented in reverse order, the response waveforms of LMCLNs changed from sinusoidal to positive ramp sawtooth shape with a fast rise and slow decay (Fig. 3F). Nevertheless, the period of the wave remained the same (Fig. 3F). In addition to the polarized light response, these two types of LMCLNs also showed a different reaction at the end of the illumination (i.e. ‘off’ response). A strong depolarizing ‘off’ response could be found in all of the polarized light-sensitive LMCLNs (Fig. 3D–F), while the others gradually repolarized towards the resting membrane potential (Fig. 3A–C).

Another type of lamina neuron was the tangential-like neurons, which could be distinguished from LMCLNs by their sustained responses to light pulses. Instead of a transient hyperpolarizing peak, the membrane potential of tangential-like neurons dropped and maintained at a steady level that resembled a sign-inversed square-wave (Fig. 3G). Furthermore, when the stimulus was turned off, the membrane potential of tangential-like neurons rose rapidly toward resting membrane potential and, in most cases, was followed by a damped oscillation (Fig. 3G,H). In particular, the post-stimulation damped oscillation was more prominent when the animal was dark-adapted and gradually diminished when it was stimulated with consecutive flashes.

CPL-sensitive cells

While targeting the lamina ganglionaris, we found three cells showing distinct responses to only R-CPL (Fig. 4). A brief pulse of white light elicited a graded depolarization plateau (Fig. 4A,D) closely resembling the response of the sign-conserving amacrine neurons of a blowfly (Douglass and Strausfeld, 2005). Under the dynamic polarization stimulus, when the polarizer moved to R-CPL, the membrane potential re-polarized as if the stimulus was fading out for a short while (Fig. 4B,C). The cell quickly resumed its depolarization potential before the status of the polarized light stimulus changed. To see whether the response was affected by the gaze angle, we moved the

Journal of Experimental Biology (2020) 223, jeb219832. doi:10.1242/jeb.219832

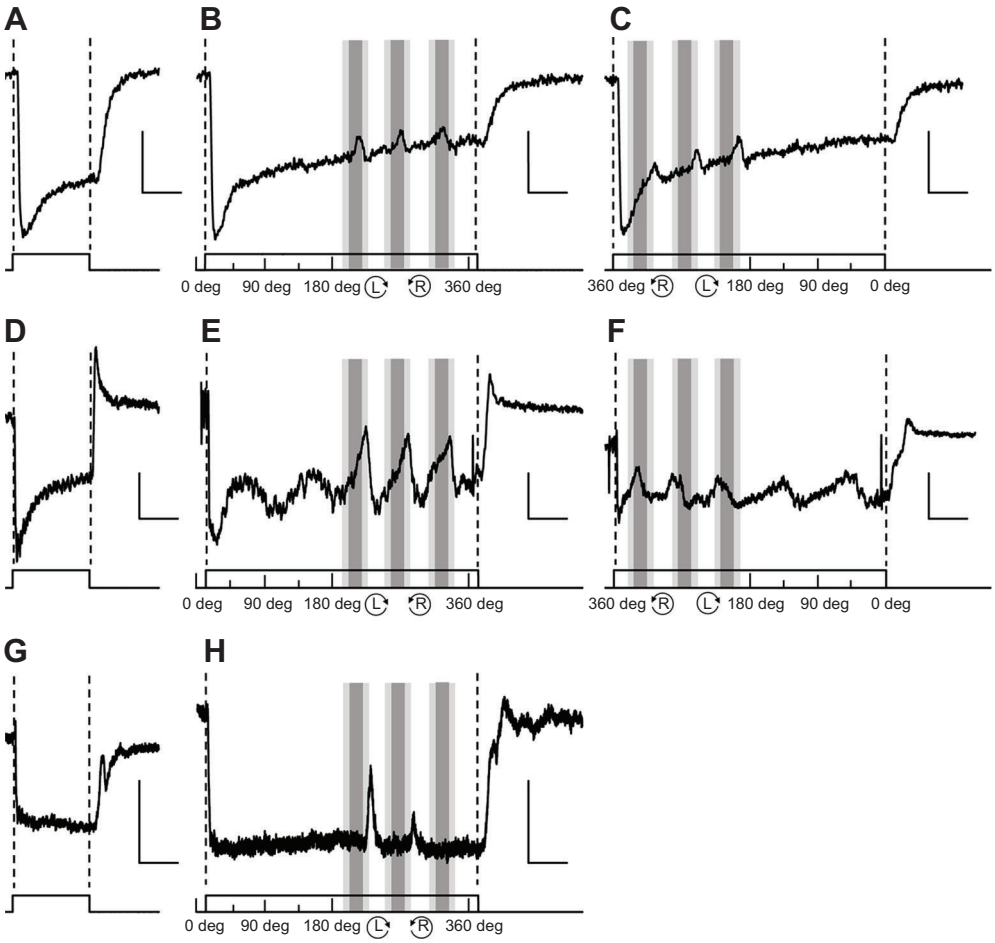

Fig. 3. Responses of lamina neurons in *H. pulchella* to light pulses and the time-varying polarized light stimuli. (A–C) Membrane potential recordings from LPL-insensitive laminar monopolar cells (LMCs) stimulated with 0.5 s light pulse (A), LPL followed by L-CPL and R-CPL (B), or R-CPL and L-CPL followed by LPL (C). (D–F) Same as A–C but acquired from polarized light-sensitive LMCs. (G–H) Voltage responses of tangential neurons to 0.5 s light pulse (G) and the sequential changing polarized light (H). The horizontal lines at the bottom of each panel indicate the status of the LED (on–off); filter details are shown below (e-vector angle of LPL or handedness of CPL). Vertical scale bars: 5 mV; horizontal scale bars: 250 ms.

light source away from the plane defined by the mid-band (i.e. stimulated from the off-axis or the edge of the receptive field). While the signal to noise ratio decreased dramatically, the response remained qualitatively the same (Fig. 4E,F). Interestingly, while the latency to on–off of the LED remained short, the membrane potential did not change when the light was temporarily blocked by the opaque tape.

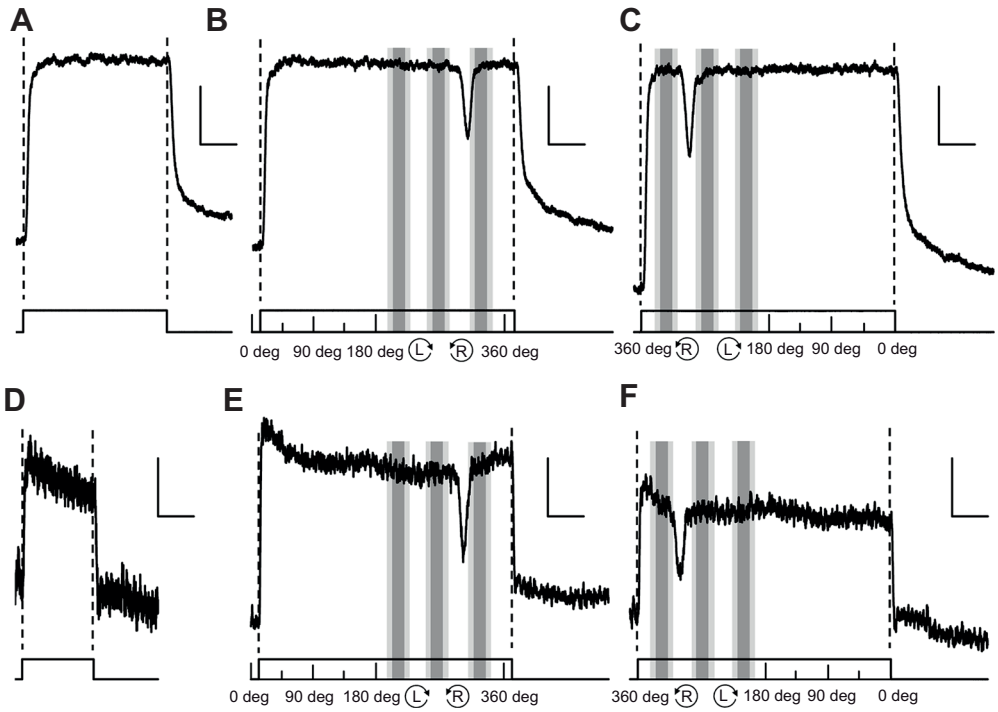

Fig. 4. Responses of CPL-sensitive neurons to the light pulses and time-varying polarized light stimuli. Graphs from left to right represent responses to different stimulus sets: (A,D) 0.5 s light pulse, (B,E) LPL followed by L-CPL and R-CPL and (C,F) R-CPL and L-CPL, followed by LPL. A–C represent responses of CPL-sensitive neurons to on-axis stimuli which were aligned with the receptive fields of the neurons. D–F show the responses when the neurons were stimulated with off-axis stimuli. Regardless of the increased noise to response ratio of responses to misaligned stimuli (D–F), the response patterns remained the same in on-axis and off-axis conditions. In both conditions, CPL-sensitive neurons showed similar graded polarizing responses to stimuli and exhibited drops in membrane potential specifically in response to R-CPL. Vertical scale bars: 2 mV in A–C and 5 mV in D–F; horizontal scale bars: 250 ms.

DISCUSSION

We found that, at the photoreceptor level, all CPL-sensitive cells in *H. pulchella* have differential responses not only to the handedness of CPL but also to the varying e-vector angles of LPL. This result supports the notion that some photoreceptors of mantis shrimp are tuned to EPL of certain ellipticity (Cronin et al., 2014; Templin et al., 2017). At the lamina, however, polarized light-sensitive neurons showed differential responses to either LPL or CPL but not both. This indicates that linearly and circularly polarized light are processed separately in the first optic lobe. These results also suggest that LPL and CPL are processed with different mechanisms. To resolve the partial polarization and/or e-vector angle of LPL, the visual system needs to compare responses from multiple receptors that differ in their preferred e-vector orientations and produce an output that represents the polarization properties (Wolff and Andreou, 1995). For decoding the handedness of CPL, however, there are only two possibilities: the cell's response should be specific to either L-CPL or R-CPL. As a result, it is not surprising to see neurons producing responses that resemble the outcome of the Boolean operation (Fig. 4).

Detection of polarized light

In addition to our electrophysiological evidence, it has been demonstrated that the mid-band rows 5 and 6 of *Haptosquilla trispinosa* and *Haptosquilla glyptocercus* are also equipped with optics that are optimized for the detection of EPL instead of CPL (Cronin et al., 2014; Templin et al., 2017). Interestingly, for all the stomatopod species examined, there is a 90 deg rotation between the ommatidia of row 5 and row 6 (Marshall et al., 1991a). Consequently, it is tempting to think that both ommatidial rows are required to analyze the handedness of CPL (Land, 2018). However, whether in row 5 or row 6, R1, R4 and R5 will always preferentially absorb L-CPL while R2, R3, R6 and R7 are more sensitive to R-CPL (Chiou et al., 2008). In other words, the role of each retinular cell is duplicated in mid-band rows 5 and 6. Even if the retardance is not exactly 1/4 λ, as long as the retardance remains the same, these four sets of photoreceptors (two sets each in two mid-band rows) are still a dual-channel system. If any other photoreceptors are involved in the detection of polarized light as a third channel, to prevent false polarization perception due to mismatched spectral absorbance, they most likely are R1–7 from hemisphere ommatidia. Alternatively, using a two-channel system, *Haptosquilla* spp. may live with a CPL detection system that may not be able to distinguish certain EPL from LPL of a particular e-vector angle. Interestingly, behavioral studies have shown that *H. trispinosa* seemed to prefer right-handed EPL over left-handed EPL or unpolarized light (Templin, 2017). Although a relatively rare occurrence (3 out of 22), in the lamina, we have found cells which showed a distinct response to R-CPL but not to L-CPL (Fig. 4). Superficially, it would appear that the objects *Haptosquilla* spp. are looking for in the environment might contain right-handed EPL or CPL. Nevertheless, they do have photoreceptors for EPL of both handedness (Fig. 2C,D). Cells that respond to R-CPL could arise from comparing either one of the circular channels with a linear or even a polarization-insensitive one. Until the identity of the neurons and their connection with photoreceptors is available, their involvement in CPL processing remains speculative.

Processing of LPL

When LPL-sensitive LMCLNs are stimulated with dynamic polarized light, the resulting waveforms indicate that they receive inputs from two channels with different angular maxima. Furthermore, instead of producing a response that represents the quantum catch ratio between these two channels (Bernard and Wehner, 1977), our recordings closely resemble a rectified sinusoidal wave (Fig. 3E). By definition, rectification can be achieved by taking the absolute difference between a sine wave (e.g. from a LPL-sensitive photoreceptor) and a threshold (e.g. from a polarization-insensitive photoreceptor). Alternatively, taking the maximum values between two sinusoidal waves which have a 1/2 λ phase difference between them (e.g. from an orthogonal pair of LPL-sensitive photoreceptors) could also produce a similar rectification result. The observed response profile shifted from sinusoidal to sawtooth shape when the polarizer was rotated in reverse order (Fig. 3E,F). This waveform shift suggests that at least two waves (instead of one sinusoidal and a straight line), slightly differing in their temporal properties, are involved in the production of the response observed in this LPL-sensitive LMCLN. A similar response has previously been observed in the LMCs of crayfish, where the rotational direction of the polarizer not only affects the response waveform but also causes a shift in peak response e-vector angle (Glantz, 1996). However, in mantis shrimp, the response peaks do not shift with the rotation direction of the polarizer (Fig. 3E,F). From the timing of the peak responses, it is clear that these two channels have their preferred e-vector angle perpendicular to each other. For example, in Fig. 3E,F, the preferred e-vector angle of this LMCLN is roughly 90 and 180 deg. Based on inferences from the morphology of the photoreceptors, this LMCLN is probably receiving inputs from the ventral hemisphere (Marshall et al., 1991a). It has been suggested that mantis shrimp may combine the linear polarization signals from dorsal and ventral hemispheres to form a four-channel LPL analyzer (Kleinlogel and White, 2008). While the four-channel theory still needs to be tested, it is unlikely to find such complicated processing at the early stage of visual processing. As expected, we did not find any lamina neuron responses that represent the combination of four linear polarization channels. Instead, our results support the behavioral evidence, which suggests that mantis shrimp analyze the LPL based on a two-channel system and consequently require torsional eye movement to improve polarization contrast (Daly et al., 2016).

Processing of CPL

The CPL-sensitive cells were most likely the lamina amacrines. Although we did not use dye filling, their identity could be determined on the basis of their light-induced depolarization (sign-conserving response) and their location among the neighboring neurons, which were impaled during electrode excursion. In Dipterans, lamina amacrine cells are thought to be involved in motion detection and/or lateral inhibition (Douglass and Strausfeld, 2003, 2005). Thoen et al. (2017) have identified three types of lamina amacrine cells in mantis shrimp based on neuronal morphology. Among these cells, that found in mid-band lamina cartridges has relatively short processes that barely span two to three cartridges (Thoen et al., 2017). Because the mid-band of mantis shrimp is a linear array of the spectroscopic and polariscopic analyzers (Marshall and Land, 1993a,b), the mid-band can only sample one slice of the surroundings at any given moment. Thus, it is unlikely that the mid-band amacrine cells are involved in motion detection. However, by relaying signals between or within rows 5 and 6, retinular cells and corresponding lamina cartridges, such an amacrine cell could be optimized for processing circular polarization information.

One interesting feature of the CPL-sensitive cells is that while they can respond to either turning on or off the illumination within 20 ms, their response to CPL comes with a rather long delay. On average, it took 76.0±3.5 ms (mean±s.e.m., n=8 recorded from 3 cells) for the cell membrane to start the depolarization in response to CPL. Because the mid-band was mounted vertically and different

types of the polarized light stimuli were separated by opaque tape, ommatidia from mid-band rows 5 and 6 should have received an identical stimulus. Therefore, this delay was not caused by the design of our dynamic polarized light stimulus. Instead, we propose that the delay is an inherent property of the neuron, which may prevent false signals as a result of temporal fluctuations of light intensity commonly found in the shallow underwater environment. The delay in processing can also explain why the neuron remained depolarized when the direct light path between the light source and the animal was briefly blocked by the opaque tape on the polarization filter (Fig. 3E). Nevertheless, a temporal low-pass filter based on a 76 ms delay would result in unacceptable motion blur, and is thus only suitable for certain nocturnal visual systems. Even in the mantis shrimp visual system, the low-pass filtering effect was exclusively observed in neurons responsive to CPL signals. The delay was not shown in any other recorded LPL-sensitive neurons and is potentially unique for processing CPL information.

Mantis shrimp often (up to 30% of the time) perform a unique scanning eye movement which has a notably slow angular velocity (ca. 40 deg s^{-1}), a short travel distance (7–10 deg) and limited orientation (more or less perpendicular to the mid-band) (Durham et al., 2018; Land, 1999; Land et al., 1990). If the mid-band is acquiring information during scanning eye movements, the processing delays of the CPL-sensitive neuron also suggest that a CPL target must be large enough to be detected. Based on the scanning velocity, one can calculate that a scanning mid-band has swept roughly 3 deg in 76 ms. Although it is assumed that the inter-ommatidial angle between mid-band rows is practically zero (Marshall and Land, 1993a), the acceptance angle of mid-band rows 5 and 6 ranges from 0.6 to 6.7 deg, depending on the species (Marshall and Land, 1993b). As a result, changes in the viewing angle by 3 deg could have moved the mid-band photoreceptors from one scanning line to the next. That is to say, by combining scanning eye movement with processing delay, the mantis shrimp created a spatiotemporal low-pass filter which prevents a small or brief CPL source from triggering a potentially undesired response.

Conclusion

Previous intracellular electrophysiological recordings in the visual system of stomatopods were all performed with ablated eyes. To our knowledge, no one has ever successfully recorded from visual interneurons in intact mantis shrimp until now. Using a combination of LPL and CPL, we have successfully determined the functional properties of lamina neurons of the stomatopod *H. pulchella*. Overall, our results have confirmed that, for smaller mantis shrimp species with correspondingly smaller eyes, the photoreceptors of mid-band rows 5 and 6 are not precisely tuned to either LPL or CPL, but perhaps to a specific set of EPL (Cronin et al., 2014). Although the perception of CPL at the photoreceptor level may be affected by the presence of LPL, it is compensated at the lamina and results in neurons that can reliably detect the presence of either CPL or LPL. It appears that the visual system of these stomatopods can separate LPL and CPL at the early stage of visual processing even if the photoreceptors are not precisely tuned to either polarization of light.

Acknowledgements

We thank Y.-P. Lee, C.-T. Shih and Z.-Y. Fang for helping with sample collection, and Dr A. Cheroske for reading and improving the English of the manuscript. We greatly appreciate two anonymous reviewers for their constructive comments and insightful suggestions to the manuscript. We also acknowledge the Kenting National Park, Construction and Planning Agency Ministry of the Interior, Taiwan for permission to collect animals.

Competing interests

The authors declare no competing or financial interests.

Author contributions

Conceptualization: T.-H.C.; Methodology: T.-H.C.; Software: T.-H.C.; Validation: T.-H.C.; Formal analysis: C.-W.W.; Investigation: C.-W.W.; Resources: T.-H.C.; Data curation: C.-W.W.; Writing - original draft: T.-H.C.; Writing - review & editing: C.-W.W.; Visualization: C.-W.W.; Supervision: T.-H.C.; Project administration: T.-H.C.; Funding acquisition: T.-H.C.

Funding

The funding of this research was provided, in part, by a Ministry of Science and Technology, Taiwan grant to T.-H.C. (MOST 102-2311-B006-002-MY3), and by the Ministry of Education, Taiwan, ROC Headquarters of University Advancement to the National Cheng Kung University (NCKU).

References

Bernard, G. D. and Wehner, R. (1977). Functional similarities between polarization vision and color vision. *Vision Res.* **17**, 1019-1028. doi:10.1016/0042-6989(77)90005-0

Born, M. and Wolf, E. (1999). *Principles of Optics: Electromagnetic Theory of Propagation, Interference and Diffraction of Light*. Cambridge; New York: Cambridge University Press.

Buchsbaum, G. and Gottschalk, A. (1983). Trichromacy, opponent colour-coding and optimum colour information transmission in the retina. *Proc. R. Soc. Lond. B* **220**, 89-113. doi:10.1098/rspb.1983.0090

Burnett, B. R. (1975). A new method for serially mounting resin sections (Spurr) for light microscopy. *Stain Technol.* **50**, 288-290. doi:10.3109/10520297509117074

Cartron, L., Dickel, L., Shashar, N. and Darmaillacq, A.-S. (2013). Maturation of polarization and luminance contrast sensitivities in cuttlefish (Sepia officinalis). *J. Exp. Biol.* **216**, 2039-2045. doi:10.1242/jeb.080390

Chiou, T.-H., Kleinlogel, S., Cronin, T., Caldwell, R., Loeffler, B., Siddiqi, A., Goldizen, A. and Marshall, J. (2008). Circular polarization vision in a stomatopod crustacean. *Curr. Biol.* **18**, 429-434. doi:10.1016/j.cub.2008.02.066

Cronin, T. W., Marshall, N. J., Quinn, C. A. and King, C. A. (1994). Ultraviolet photoreception in mantis shrimp. *Vision Res.* **34**, 1443-1452. doi:10.1016/0042-6989(94)90145-7

Cronin, T. W., Johnsen, S., Marshall, N. J. and Warrant, E. J. (2014). *Visual Ecology*. Princeton: Princeton University Press.

Daly, I. M., How, M. J., Partridge, J. C., Temple, S. E., Marshall, N. J., Cronin, T. W. and Roberts, N. W. (2016). Dynamic polarization vision in mantis shrimps. *Nat. Commun.* **7**, 12140. doi:10.1038/ncomms12140

Daw, N. W. (1973). Neurophysiology of color vision. *Physiol. Rev.* **53**, 571-611. doi:10.1152/physrev.1973.53.3.571

Douglass, J. K. and Strausfeld, N. J. (2003). Anatomical organization of retinotopic motion-sensitive pathways in the optic lobes of flies. *Microsc. Res. Tech.* **62**, 132-150. doi:10.1002/jemt.10367

Douglass, J. K. and Strausfeld, N. J. (2005). Sign-conserving amacrine neurons in the fly's external plexiform layer. *Vis. Neurosci.* **22**, 345-358. doi:10.1017/S095252380522309X

Durham, M. F., Lin, C. and Cronin, T. W. (2018). Scanning eye movements of the stomatopod crustacean, Neogonodactylus oerstedii, in polarized light fields. *Mar. Freshw. Behav. Physiol.* **51**, 263-273. doi:10.1080/10236244.2018.1543544

Freifeld, L., Clark, D. A., Schnitzer, M. J., Horowitz, M. A. and Clandinin, T. R. (2013). GABAergic lateral interactions tune the early stages of visual processing in Drosophila. *Neuron* **78**, 1075-1089. doi:10.1016/j.neuron.2013.04.024

Gagnon, Y. L., Templin, R. M., How, M. J. and Marshall, N. J. (2015). Circularly polarized light as a communication signal in mantis shrimps. *Curr. Biol.* **25**, 3074-3078. doi:10.1016/j.cub.2015.10.047

Glantz, R. M. (1996). Polarization sensitivity in the crayfish optic lobe: peripheral contributions to opponency and directionally selective motion detection. *J. Neurophysiol.* **76**, 3404-3414. doi:10.1152/jn.1996.76.5.3404

Glantz, R. M. and Bartels, A. (1994). The spatiotemporal transfer function of crayfish lamina monopolar neurons. *J. Neurophysiol.* **71**, 2168-2182. doi:10.1152/jn.1994.71.6.2168

Glantz, R. M. and Schroeter, J. P. (2006). Polarization contrast and motion detection. *J. Comp. Physiol. A* **192**, 905-914. doi:10.1007/s00359-006-0127-4

Horváth, G. (2014). *Polarized Light and Polarization Vision in Animal Sciences*, 2nd edn. Springer Science and Business Media.

How, M. J., Porter, M. L., Radford, A. N., Feller, K. D., Temple, S. E., Caldwell, R. L., Marshall, N. J., Cronin, T. W. and Roberts, N. W. (2014). Out of the blue: the evolution of horizontally polarized signals in Haptosquilla (Crustacea, Stomatopoda, Protosquillidae). *J. Exp. Biol.* **217**, 3425-3431. doi:10.1242/jeb.107581

Ivanoff, A. and Waterman, T. H. (1958). Elliptical polarization of submarine illumination. *J. Mar. Res.* **16**, 255-282.

Johnsen, S. N. (2012). *The Optics of Life: a Biologist's Guide to Light in Nature*. Princeton, NJ: Princeton University Press.

Kleinlogel, S. and White, A. G. (2008). The secret world of shrimps: polarisation vision at its best. *PLoS ONE* **3**, e2190. doi:10.1371/journal.pone.0002190
Land, M. F. (1999). Motion and vision: why animals move their eyes. *J. Comp. Physiol. A* **185**, 341-352. doi:10.1007/s003590050393
Land, M. F. (2018). *Eyes to See: The Astonishing Variety of Vision in Nature*. Oxford, United Kingdom: Oxford University Press.
Land, M. F., Marshall, N. J., Brownless, D. and Cronin, T. W. (1990). The eye-movements of the mantis shrimp *Odontodactylus scyllarus* (Crustacea: Stomatopoda). *J. Comp. Physiol. A* **167**, 155-166. doi:10.1007/BF00188107
Laughlin, S. B. and Osorio, D. (1989). Mechanisms for neural signal enhancement in the blowfly compound eye. *J. Exp. Biol.* **144**, 113-146.
Manning, R. B., Schiff, H. and Abbott, B. C. (1984). Cornea shape and surface structure in some stomatopod crustacea. *J. Crust. Biol.* **4**, 502-513. doi:10.2307/1548046
Marshall, N. J. and Cronin, T. W. (2014). Polarisation Vision of Crustaceans. In *Polarized Light and Polarization Vision in Animal Sciences*, (ed. G. Horváth), pp. 171-216. Springer.
Marshall, N. J. and Land, M. F. (1993a). Some optical features of the eyes of stomatopods. I. Eye shape, optical axis and resolution. *J. Comp. Physiol. A* **173**, 565-582. doi:10.1007/BF00197765
Marshall, N. J. and Land, M. F. (1993b). Some optical features of the eyes of stomatopods. II. Ommatidial design, sensitivity and habitat. *J. Comp. Physiol. A* **173**, 583-594. doi:10.1007/BF00197766
Marshall, N. J., Land, M. F., King, C. A. and Cronin, T. W. (1991a). The compound eyes of mantis shrimps (Crustacea, Hoplocarida, Stomatopoda). I. Compound eye structure: the detection of polarised light. *Phil. Trans. R. Soc. Lond. B* **334**, 33-56. doi:10.1098/rstb.1991.0096
Marshall, N. J., Land, M. F., King, C. A. and Cronin, T. W. (1991b). The compound eyes of mantis shrimps (Crustacea, Hoplocarida, Stomatopoda). II. Colour pigments in the eyes of stomatopod crustaceans: polychromatic vision by serial and lateral filtering. *Phil. Trans. R. Soc. Lond. B* **334**, 57-84. doi:10.1098/rstb.1991.0097
Moody, M. F. and Parriss, J. R. (1961). The discrimination of polarised light by *Octopus:* a behavioural and morphological study. *Z. Vergl. Physio.* **44**, 268-291. doi:10.1007/BF00298356
Nilsson, D. E. and Warrant, E. J. (1999). Visual discrimination: Seeing the third quality of light. *Curr. Biol.* **9**, R535-537. doi:10.1016/S0960-9822(99)80330-3
Pignatelli, V., Temple, S. E., Chiou, T.-H., Roberts, N. W., Collin, S. P. and Marshall, N. J. (2011). Behavioural relevance of polarization sensitivity as a target detection mechanism in cephalopods and fishes. *Philos. Trans. R. Soc. Lond. B* **366**, 734-741. doi:10.1098/rstb.2010.0204
Porter, M. L., Zhang, Y., Desai, S., Caldwell, R. L. and Cronin, T. W. (2010). Evolution of anatomical and physiological specialization in the compound eyes of stomatopod crustaceans. *J. Exp. Biol.* **213**, 3473-3486. doi:10.1242/jeb.046508
Roberts, N. W., Chiou, T.-H., Marshall, N. J. and Cronin, T. W. (2009). A biological quarter-wave retarder with excellent achromaticity in the visible wavelength region. *Nat. Photonics* **3**, 641-644. doi:10.1038/nphoton.2009.189
Schwind, R. (1984). Evidence for true polarization vision based on a two-channel analyzer system in the eye of the water bug,Notonecta glauca. *J. Comp. Physiol. A* **154**, 53-57. doi:10.1007/BF00605390
Snyder, A. W. (1973). Polarisation sensitivity of individual retinula cells. *J. Comp. Physiol.* **83**, 331-360. doi:10.1007/BF00696351
Temple, S. E., Pignatelli, V., Cook, T., How, M. J., Chiou, T.-H., Roberts, N. W. and Marshall, N. J. (2012). High-resolution polarisation vision in a cuttlefish. *Curr. Biol.* **22**, R121-R122. doi:10.1016/j.cub.2012.01.010
Temple, S. E., McGregor, J. E., Miles, C., Graham, L., Miller, J., Buck, J., Scott-Samuel, N. E. and Roberts, N. W. (2015). Perceiving polarization with the naked eye: characterization of human polarization sensitivity. *Proc. R. Soc. Lond. B* **282**, 20150338. doi:10.1098/rspb.2015.0338
Templin, R. (2017). Circular polarization vision in stomatopod crustaceans. *PhD thesis*, Queensland Brain Institute, University of Queensland, 127pp.
Templin, R. M., How, M. J., Roberts, N. W., Chiou, T.-H. and Marshall, J. (2017). Circularly polarized light detection in stomatopod crustaceans: a comparison of photoreceptors and possible function in six species. *J. Exp. Biol.* **220**, 3222-3230. doi:10.1242/jeb.162941
Thoen, H. H., How, M. J., Chiou, T.-H. and Marshall, J. (2014). A different form of color vision in mantis shrimp. *Science* **343**, 411-413. doi:10.1126/science.1245824
Thoen, H. H., Sayre, M. E., Marshall, J. and Strausfeld, N. J. (2018). Representation of the stomatopod's retinal midband in the optic lobes: putative neural substrates for integrating chromatic, achromatic and polarization information. *J. Comp. Neurol.* **526**, 1148-1165. doi:10.1002/cne.24398
Thoen, H. H., Strausfeld, N. J. and Marshall, J. (2017). Neural organization of afferent pathways from the stomatopod compound eye. *J. Comp. Neurol.* **525**, 3010-3030. doi:10.1002/cne.24256
Wang-Bennett, L. T. and Glantz, R. M. (1987a). The functional organization of the crayfish *Lamina ganglionaris*. I. Nonspiking monopolar cells. *J. Comp. Physiol. A* **161**, 131-145. doi:10.1007/BF00609461
Wang-Bennett, L. T. and Glantz, R. M. (1987b). The functional organization of the crayfish lamina ganglionaris. II. Large-field spiking and nonspiking cells. *J. Comp. Physiol. A* **161**, 147-160. doi:10.1007/BF00609462
Wolff, L. B. and Andreou, A. G. (1995). Polarization camera sensors. *Image Vision Comput.* **13**, 497-510. doi:10.1016/0262-8856(95)94383-B